ACCOUNTS
of chemical research

Combination of Lightweight Elements and Nanostructured Materials for Batteries

JUN CHEN* AND FANGYI CHENG

Institute of New Energy Material Chemistry and Engineering Research Center of Energy Storage & Conversion (Ministry of Education), Chemistry College, Nankai University, Tianjin 300071, China

RECEIVED ON OCTOBER 13, 2008

CONSPECTUS

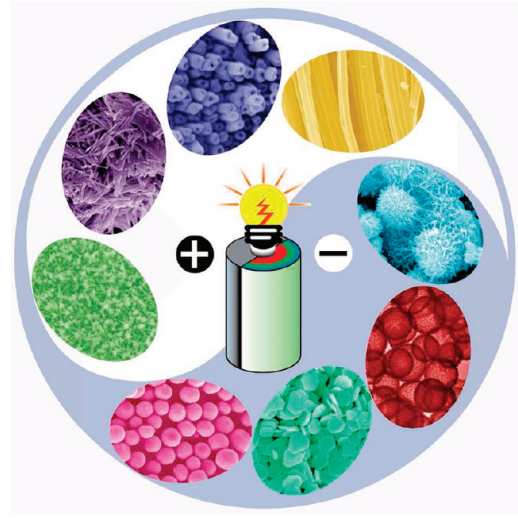

In a society that increasingly relies on mobile electronics, demand is rapidly growing for both primary and rechargeable batteries that power devices from cell phones to vehicles. Existing batteries utilize lightweight active materials that use electrochemical reactions of ions such as H^+, OH^- and Li^+/Mg^{2+} to facilitate energy storage and conversion. Ideal batteries should be inexpensive, have high energy density, and be made from environmentally friendly materials; batteries based on bulk active materials do not meet these requirements. Because of slow electrode process kinetics and low-rate ionic diffusion/migration, most conventional batteries demonstrate huge gaps between their theoretical and practical performance.

Therefore, efforts are underway to improve existing battery technologies and develop new electrode reactions for the next generation of electrochemical devices. Advances in electrochemistry, surface science, and materials chemistry are leading to the use of nanomaterials for efficient energy storage and conversion. Nanostructures offer advantages over comparable bulk materials in improving battery performance.

This Account summarizes our progress in battery development using a combination of lightweight elements and nanostructured materials. We highlight the benefits of nanostructured active materials for primary zinc−manganese dioxide (Zn−Mn), lithium−manganese dioxide (Li−Mn), and metal (Mg, Al, Zn)−air batteries, as well as rechargeable lithium ion (Li-ion) and nickel−metal hydride (Ni−MH) batteries. Through selected examples, we illustrate the effect of structure, shape, and size on the electrochemical properties of electrode materials. Because of their numerous active sites and facile electronic/ionic transfer and diffusion, nanostructures can improve battery efficiency.

In particular, we demonstrate the properties of nanostructured active materials including Mg, Al, Si, Zn, MnO_2, CuV_2O_6, $LiNi_{0.8}Co_{0.2}O_2$, $LiFePO_4$, Fe_2O_3, Co_3O_4, TiS_2, and $Ni(OH)_2$ in battery applications. Electrochemical investigations reveal that we generally attain larger capacities and improved kinetics for electrode materials as their average particle size decreases. Novel nanostructures such as nanowires, nanotubes, nanourchins, and porous nanospheres show lower activation energy, enhanced reactivity, improved high-rate charge/discharge capability, and more controlled structural flexibility than their bulk counterparts. In particular, anode materials such as Si nanospheres and Fe_2O_3 nanotubes can deliver reversible capacity exceeding 500 mA·h/g. (Graphite used commercially has a theoretical capacity of 372 mA·h/g.) Nanocomposite cathode materials such as NiP-doped $LiFePO_4$ and metal hydroxide-coated $Ni(OH)_2$ nanotubes allow us to integrate functional components, which enhance electrical conductivity and suppress volume expansion. Therefore, shifting from bulk to nanostructured electrode materials could offer a revolutionary opportunity to develop advanced green batteries with large capacity, high energy and power density, and long cycle life.

Published on the Web 04/08/2009 www.pubs.acs.org/acr
10.1021/ar800229g CCC: $71.50

1. Introduction

Both primary and rechargeable batteries, which can generate clean electric energy from the stored chemical energy through the desired electrochemical reactions, are essential to the convenience and sustainability of human development in the modern mobile society.[1] Batteries cover a wide scope of applications independent of utility power, ranging from portable consumer electronic devices to electric vehicles.[2] The main issues facing various current batteries are the slow electrode-process kinetics with large polarization and low rate of ionic diffusion/migration, resulting in limited practical energy output and battery performance. Nowadays, efforts in battery research and development are devoted to energy storage and conversion with high efficiency, high energy density, environmental friendliness, and low cost.

The capacity (Q) and voltage (E) of a battery are theoretically determined by the electrode reactions according to the Faraday equation and Gibbs free energy change (ΔG): $Q = nF/M$ and $\Delta G = nFE$, where n is the number of electrons involved in stoichiometric reaction, F is the Faraday constant, and M is the equivalent molecular weight.[3] Generally, electrode materials based on lightweight elements can deliver large capacity and high potential. Such representative batteries include primary zinc−manganese dioxide (Zn−Mn), lithium−manganese dioxide (Li−Mn), and metal−air batteries, as well as rechargeable lithium ion (Li-ion) and nickel−metal hydride (Ni−MH) batteries.[2] These batteries utilize lightweight active materials that enable the transfer of lightweight ions such as H^+, OH^-, and Li^+ through the desired electrochemical reactions (Figure 1). Despite great success, there are still many obstacles for portable applications of traditional batteries in new-generation electronic devices and automobiles due to the disadvantages of low energy and power density, short service life, and high production cost.

The emerging nanoscience and nanotechnology offer a revolutionary opportunity to fulfill the goals of efficient and clean energy utilization. During the past two decades, nanoscale materials have shown peculiar physical and chemical properties differing from their bulk counterparts.[4,5] Using nanomaterials has opened up a new avenue to enhance the electrochemical reactivity and to improve the efficiency of energy storage and conversion devices.[6−8] When employed in batteries, nanostructured active materials may outperform the corresponding bulk form because they facilitate more efficient electronic/ionic diffusion, provide more active sites, enhance structural flexibility, and allow new reaction mechanisms.[9,10] In this Account, we will summarize our progress in battery development using the combination of lightweight elements and nanostructured materials. The main scope highlights the difference in the electrode kinetics and performance among nano, meso, and bulk active materials that are used in aqueous-electrolyte-based Zn−Mn, Mg−Air, and Ni−MH batteries, as well as nonaqueous lithium batteries.

Zn-Mn	(−) $Zn + 2OH^- \rightarrow Zn(OH)_2 + 2e$	$\varphi^\circ = -1.25$ V	(1)
	(+) $MnO_2 + H_2O + e^- \rightarrow MnOOH + OH^-$	$\varphi^\circ = 0.36$ V	(2)
	(o) $Zn + 2MnO_2 + 2H_2O \rightarrow Zn(OH)_2 + MnOOH$	$E^\circ = 1.61$ V	(3)
Li-Mn	(−) $xLi \rightarrow xLi^+ + xe$	$\varphi^\circ = -3.01$ V	(4)
	(+) $MnO_2 + xLi^+ + xe^- \rightarrow Li_xMnO_2$	$\varphi^\circ = 0.49$ V	(5)
	(o) $MnO_2 + xLi \rightarrow Li_xMnO_2$	$E^\circ = 3.50$ V	(6)
Zn-air	(−) $Zn + 2OH^- \rightarrow ZnO + H_2O + 2e$	$\varphi^\circ = -1.25$ V	(7)
	(+) $O_2 + 2H_2O + 4e \rightarrow 4OH^-$	$\varphi^\circ = 0.40$ V	(8)
	(o) $2Zn + O_2 \rightarrow 2ZnO$	$E^\circ = 1.65$ V	(9)
Li-ion	(−) $Li_xC \rightarrow C + xLi^+ + xe$	$\varphi^\circ = -2.90$ V	(10)
	(+) $Li_{1-x}CoO_2 + xLi^+ + xe \rightarrow LiCoO_2$	$\varphi^\circ = 1.20$ V	(11)
	(o) $Li_xC + Li_{1-x}CoO_2 \rightarrow C + LiCoO_2$	$E^\circ = 4.10$ V	(12)
Ni-MH	(−) $MH + OH^- \rightarrow M + H_2O + e$	$\varphi^\circ = -0.83$ V	(13)
	(+) $NiOOH + H_2O + e \rightarrow Ni(OH)_2 + OH^-$	$\varphi^\circ = 0.49$ V	(14)
	(o) $MH + NiOOH \rightarrow M + Ni(OH)_2$	$E^\circ = 1.32$ V	(15)

FIGURE 1. Electrochemical reactions involved in the representative lightweight-elements batteries.

2. Primary Batteries

Primary batteries are simple and convenient portable power sources for various applications including lighting, medical devices, military facilities, etc. Alkaline Zn−Mn batteries have taken over most of the current primary battery market, and their production and consumption continue to grow because of their advantageous cost and performance. Meanwhile, much progress has also been made in developing primary metal−air and lithium batteries, which employ light metals as the anode.[2] Lithium is the lightest metal and may deliver a theoretical capacity up to 3860 mA·h/g. Because lithium plating may cause short-circuit problem in batteries, magnesium is an alternative lightweight element with lower cost, lower toxicity, and higher safety. Also, Mg is abundant in both the earth's crust and seawater. Similarly, other active metals such as aluminum and zinc are attractive electrode materials with high capacity (theoretically 2980 and 820 mA·h/g for Al and Zn, respectively). However, the practical capacity of the employed active materials for primary batteries remains limited due to low utilization efficiency of the traditional bulk form. Recent development in nanostructured materials helps to address the capacity issue and make their applications in batteries possible. Here we demonstrate the synthesis and characterization of nanostructured MnO_2, vanadate, and active

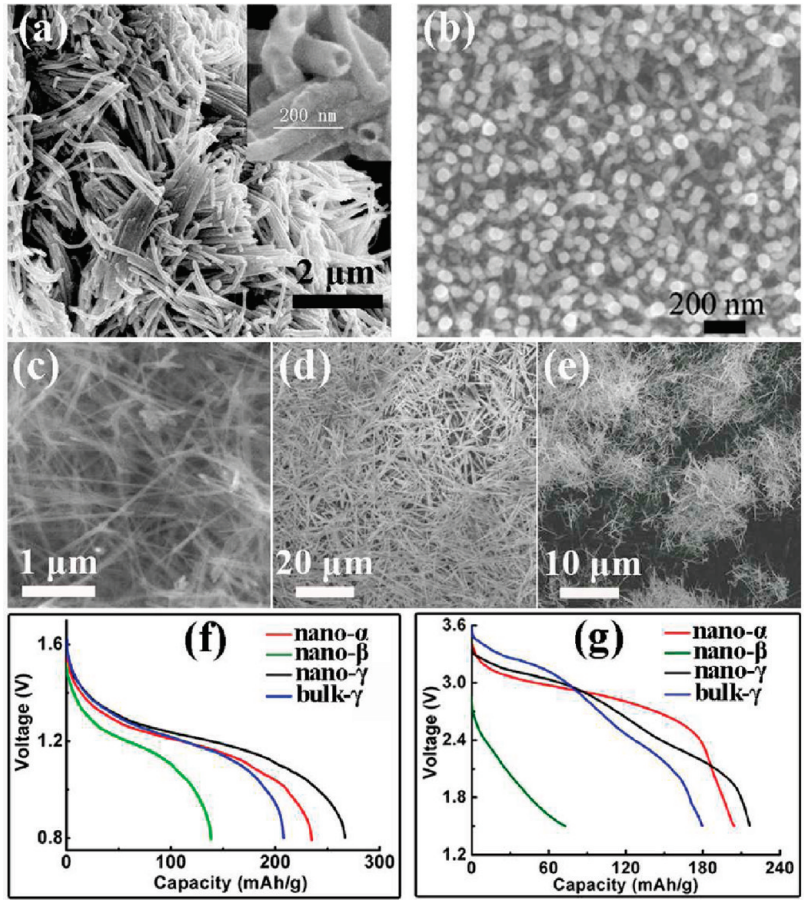

FIGURE 2. Morphologies and electrochemical properties of MnO_2 nanostructures: SEM images of (a) γ-MnO_2 nanotubes/nanowires, (b) film composed of γ-MnO_2 nanorods, and nanowires of (c) α-MnO_2, (d) β-MnO_2, and (e) γ-MnO_2; discharge curves of bulk and nanostructured MnO_2 in (f) Zn−Mn and (g) Li−Mn batteries.

metals and their superior performance when compared with their bulk counterparts.

2.1. MnO_2 Nanostructures. Manganese oxides have versatile applications in catalysis and magnetism due to their compositional, structural, and morphological diversity.[11] MnO_2 exists in various forms (with tunnels, layers, and spinel structures) when the structural units (MnO_6 octahedra) are linked in different ways.[12] MnO_2 can be applied as cathode materials for both Zn−Mn and Li−Mn primary batteries. The crystallographic structure and morphology strongly affect its electrode performance since intercalation or extraction of protons or Li^+ into or from the MnO_2 lattice determines the kinetics of electrode reaction (Figure 1, eqs 2 and 5).[13]

The preparation of MnO_2 nanomaterials with controlled structure and shape has been achieved through a solution route.[14] In our group, one-dimensional (1D) nanostructured γ-MnO_2 samples containing nanotubes and nanowires (Figure 2a) were prepared through a surfactant-assisted hydrothermal route.[15] Thin films consisting of γ-MnO_2 nanorods (Figure 2b) were fabricated by combining potentiostatic and cyclic voltammetric electrodeposition techniques.[16] The film texture was controlled by adjusting electrodeposition parameters such as deposition time and potential scanning rate. It is worth noting that electrodeposited γ-MnO_2 on a metal substrate can be directly employed as an electrode to assemble thin-film batteries or supercapacitors, thus avoiding the use of additive components such as conducting and binding agents. To evaluate the influence of crystal structure and morphology on electrochemical properties, α-, β-, and γ-MnO_2 nanostructures (Figure 2c−e) were obtained from simple hydrothermal treatment of Mn(II) species without any template.[17] The discharge curves (Figure 2f,g) clearly show that nanostructures are superior to the comparative bulk form. For example, γ-MnO_2 nanowires deliver a high capacity of 267 mA·h/g in a Zn−Mn laboratory cell and a considerable high capacity exceeding 210 mA·h/g in a Li−Mn cell, which correspond to an increase of 28% and 17% in comparison with the values of the bulk γ-MnO_2, respectively.

Among the three phases, β-MnO_2 possesses only narrow (1 × 1) tunnels, which are unfavorable for proton and Li^+ diffu-

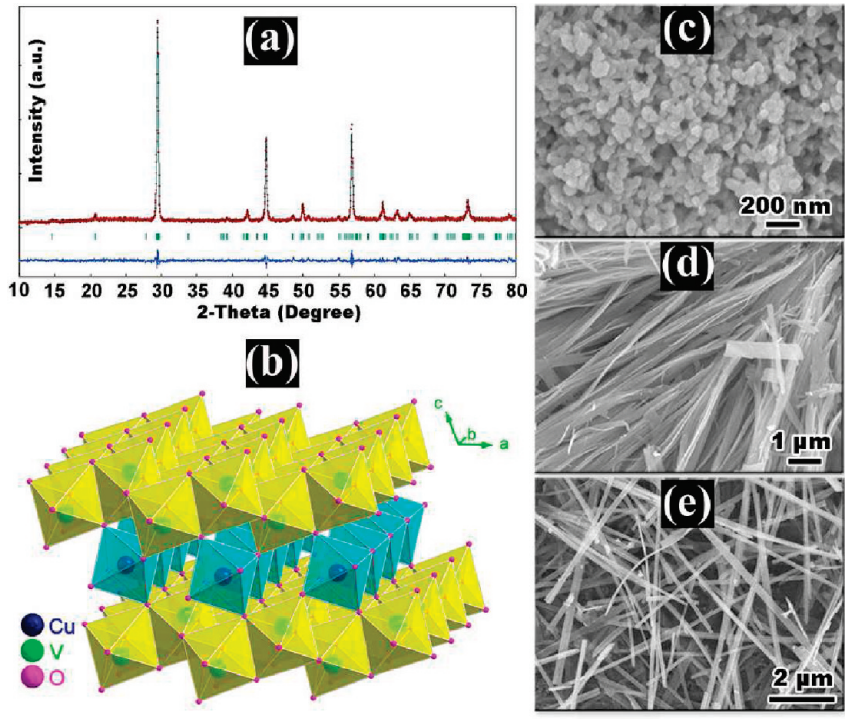

FIGURE 3. (a) Rietveld refinement of XRD patterns, (b) crystal structure of CuV_2O_6 nanowires, and (c−e) SEM images showing the morphological evolvement during the hydrothermal synthesis of CuV_2O_6.

sion; whereas the larger (1 × 2) tunnels present in γ-MnO_2 favor the insertion and transfer of ions in the lattice framework, leading to the high activity.[12,13] Accordingly, the prepared β-MnO_2 samples exhibit poor performance in terms of low potential and capacity. However, a recent study reported that reversible lithium intercalation was realized in the ordered mesoporous β-MnO_2, owing to the fact that its high surface areas and interconnected porous nanostructure could better accommodate structural changes.[18] This example demonstrated the power of using nanostructures to modify electrode materials that were traditionally perceived to be inactive. For the hollandite-type α-MnO_2 grown by a solution-based process, cations and small molecules such as NH_4^+, K^+, or H_2O reside in the large (2 × 2) channels as template to stabilize the framework, as evidenced by elemental and thermal analysis.[19] These stabilizing bulky items may impede ionic diffusion and intercalation, thus limiting the electrode performance to some extent.[13]

2.2. Vanadate Nanowires. There is increasing demand for power sources for implantable medical devices (e.g., cardioverter defibrillators), which require long-term stability and high energy density. Currently, the primary choice for this purpose is lithium batteries constructed with mixed metal vanadium oxides such as $Ag_2V_4O_{11}$ and $Ag_4V_2O_6F_2$.[20] The vanadates, which possess layered structure for lithium insertion/intercalation (e.g., α-CuV_2O_6 consists of VO_6 octahedral double layers separated by CuO_6 octahedral chains, as shown in Figure 3b), can deliver high capacity over 2.0 V due to multistep reduction of mixed-valence transition metals.

Traditional energy-consuming synthesis of these vanadates by high-temperature solid-state techniques generally yields product with irregular shape or large particle size. To better control the shape and size, we have synthesized a series of 1D micro- to nanostructured transition metal vanadates including $Ag_2V_4O_{11}$, $AgVO_3$, and CuV_2O_6.[21,22] Our preparation of vanadate nanostructures followed a hydrothermal route from the reactions of dissolvable metal salts and ammonium metavanadate. For instance, the synthesis of α-CuV_2O_6 nanowires undergoes an Ostwald ripening and splitting process that can be divided into three stages: the initial nuclei formation and aggregation to produce $Cu_3(OH)_2V_2O_7 \cdot 2H_2O$ nanoparticles (Figure 3c), the growth of particles to lamellar microstructure (Figure 3d), and the splitting of the layered structure into the final CuV_2O_6 nanowires (Figure 3e) through phase transformation.[22] The obtained nanomaterials are of high crystalline purity, as revealed by Rietveld refinement of the XRD pattern (Figure 3a).

Investigations of vanadate materials for primary lithium batteries clearly revealed morphology-dependent performance. In the case of α-CuV_2O_6, all discharge profiles (Figure 4a) display similar shape with distinguishable sloping voltage plateaus being ascribed to the reduction of Cu and V at

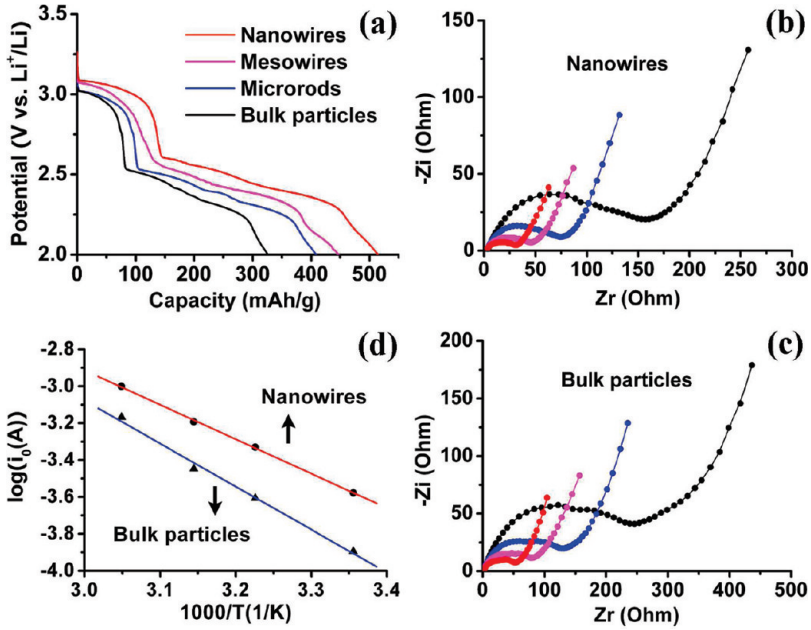

FIGURE 4. Electrochemical properties of CuV_2O_6 for primary lithium batteries: (a) discharge curves, (b, c) EIS at different temperatures (black, blue, magenta, and red denote 25, 37, 45, and 55 °C, respectively), and (d) Arrhenius plots.

different potential ranges.[22] The capacity increases in the order of bulk particles < microrods < mesowires < nanowires. A notable discharge capacity exceeding 500 mA·h/g is attained for α-CuV_2O_6 nanowires. Interestingly, the open circuit voltages and voltage plateaus also show an increasing trend from bulk to nanosize. This trend can be interpreted by reduced electrode polarization and size effect on energetics due to the contribution of excess surface free energy.[23] Electrochemical impedance spectra (EIS, Figure 4b,c) at constant potential confirm that nanowires attain lower charge transfer resistance (R_{ct}) than the bulk counterparts. The exchange current (i_0) and the apparent activation energy (E_a) for lithium intercalation can be calculated from the equation $i_0 = RT/(nFR_{ct}) = A\exp(-E_a/(RT))$, where A is a temperature-independent coefficient, R is the universal gas constant, and T is the absolute temperature.[3] The activation energy at 2.3 V is 35.7 and 44.6 kJ/mol for nanowires and bulk particles, respectively, as determined from the Arrhenius plots (Figure 4d). Therefore, enhancement of reactivity and kinetics arising from shorter Li-ion diffusion distance and larger surface areas is obviously achieved as particle size decreases.

2.3. Mg, Al, and Zn Micro- and Nanostructures. Light active metals such as Mg, Al, and Zn have been widely utilized as anode materials. However, their intrinsic problem of passivation and corrosion severely limits their practical voltage and Coulombic efficiency. Moving from traditional bulk to nanoscale materials offers a new solution to overcome such obstacles. The passivation layer formed on metal nanostructures dissolves more easily in electrolyte because of the resulting higher reactivity. In addition, the high electrochemically active surface areas of nanomaterials lower the real current density and thus reduce the electrode polarization. We have investigated the electrode characteristics of active metals with micro-, meso-, and nanoscale structures.[24−26] Various metallic Mg, Al, and Zn structures have been prepared via a simple vapor-transport approach, which involves procedures of evaporating commercial metal powders, transporting gaseous metal, and depositing metal samples on substrate. Size and shape control is achievable by adjusting the experimental parameters such as the evaporation or deposition temperature and the flow rate of carrier gas.

As an illustrative example, Figure 5 shows the morphologies and properties of Mg samples with shapes of spheres (A), plates (B), nanorods (C), and urchin-like nanostructures (D).[25] Because Mg is highly reactive in alkaline aqueous solution, we have applied a moderate electrolyte containing $Mg(NO_3)_2$ and $NaNO_2$ solution to reduce the polarization and self-discharge. The starting potential of Mg anodic dissolution is approximately 0.1 V more negative for Mg nano- or mesostructures than for the bulk Mg powders (Figure 5e). In addition, the anodic dissolution current density increases from bulk to nanostructures. Furthermore, the Mg−air batteries assembled with sample D exhibit higher discharge voltage and longer discharge time than those with sample A (Figure 5f). Thus, the electrochemical activity of the Mg anode is highly dependent on its shape and size. The urchin-like nanostructures

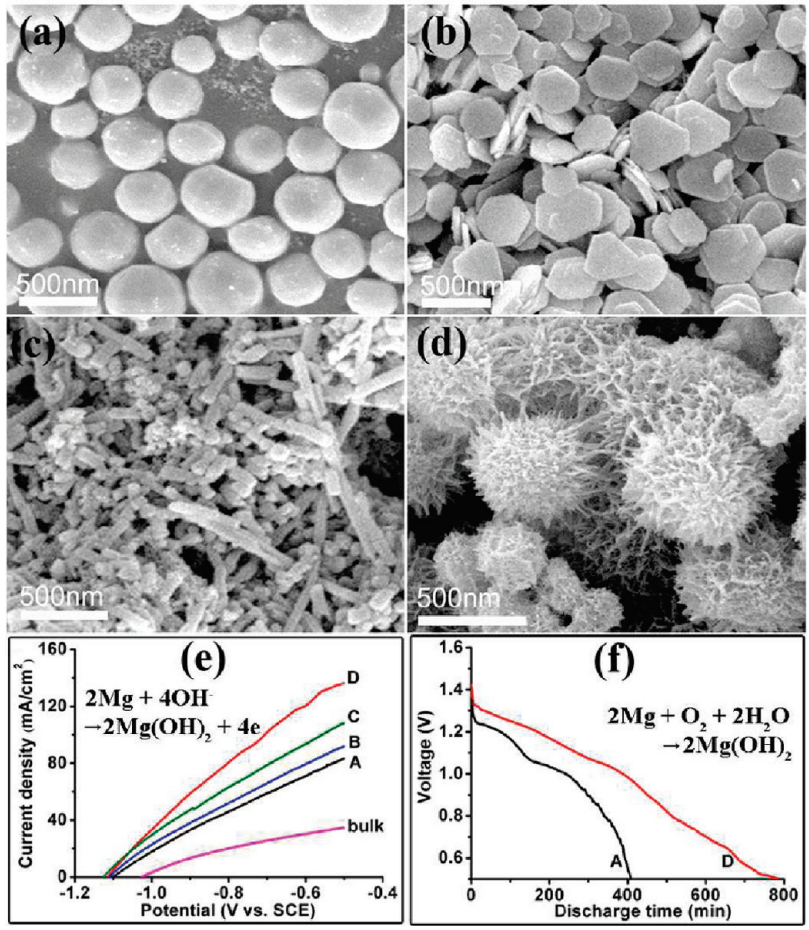

FIGURE 5. (a–d) SEM images of Mg samples A, B, C, and D, respectively, (e) linear sweep voltammograms, and (f) discharge curves of the laboratory Mg–air batteries.

greatly benefit from low anodic polarization and fast sedimentation of the anodic product (i.e., $Mg(OH)_2$) in electrolyte, owing to the small size, large surface areas, and porous interconnected network.

We have employed the Mg, Al, and Zn nanostructures as anode active materials in metal–air and Zn–Mn batteries. The assembled laboratory Mg–air cell based on urchin-like Mg and fluid electrolyte delivered an energy density of 565 W·h/kg.[24] The Al–air cell with Al nanorods and KOH/ethanol electrolyte exhibited an energy density of 572 W·h/kg.[26] Practical energy density of 157 W·h/kg was obtained for a Zn–Mn cell with Zn nanospheres.[25] Additionally, these three types of batteries showed favorable high-rate discharge ability. In general, the nanostructure-based batteries exhibited at least 20% larger capacities and higher energy densities compared with the bulk-based batteries. These results provide evidence for the huge potential of applying nanostructured active metals as anode materials to construct high-power primary batteries.

3. Rechargeable Batteries

Rechargeable batteries are currently prevailing portable power sources because they are material saving due to repeated charge and discharge. Nowadays, the environmental awareness and high energy density demand lead to the popularity of Li ion and Ni–MH batteries, which have gradually become an alternative power source to traditional lead–acid and Ni–Cd batteries.[1] Li ion batteries are extensively used in high-end consumer electronics, while Ni–MH batteries are widely used to power less expensive electronic devices. Further development of advanced rechargeable batteries is stringent to meet the wide applications of three typical categories: the ever-expanding 3C (computer, communication, and consumer electronics) devices, the energy storage devices for solar and other renewable energy, and the emerging electric automobiles.[2]

3.1. Nanostructures for Li Ion Batteries. Current research and development of Li ion batteries can hardly keep

up with the growing demand of the ever-increasing 3C market. New-generation wireless communication technologies require batteries with lighter weight, higher energy/power density, and longer cycle life. Commercial Li ion batteries generally utilize classic Li^+ intercalation compounds ($LiCoO_2$) and carbons as active materials (Figure 1, eqs 10−12), which fall in short with limited inherent capacity.[27] Switching from bulk to nanostructured electrodes will lead to revolutionary advance of battery performance, especially with respect to capacity and high-rate capability.[6,7] Nanomaterials, providing higher reactivity and short diffusion length for Li ions, enable researchers to either modify existing electrodes or develop a new lithium reactivity concept.

The cathode materials in use for current Li ion batteries mainly include lithiated transition metal oxides. Practically, reversible Li intercalation/extraction can be carried out merely in a limited range of composition, due to the high oxidizing reactivity of the almost delithiated metal oxide with organic electrolyte.[27] Besides, the phase transition and Jahn−Teller driven structural distortion may cause capacity fade. Nanostructures are not likely to suppress the structural change, but rather, they can accommodate better the strains related to this transformation. Moreover, the short Li^+ diffusion in nanocrystalline materials would significantly improve the high-rate capability. On the other side, the large surface area of nanomaterials may incur undesired side reactions with the electrolyte, particularly at high voltages or temperatures.[6] This would inevitably result in poor cyclability. The solution to this problem is to adopt nanoarchitectured materials that possess external particle size at micro- or mesoscale while internally maintaining nanosized grains.[9]

Template-directed nanotubes (Figure 6a) are an example of this kind of nanoarchitecture. The nanotubes have an average diameter of around 200 nm and length of several micrometers. The walls of the tubes are composed of nanoparticles with sizes of 10−40 nm. Moreover, this particle size falls in the range that is found to be favorable for practical application.[28] Therefore, the tubular architectures are anticipated to reduce side reactions while maintaining nanosize effect benefits. Indeed, $LiCoO_2$, $LiNi_{0.8}Co_{0.2}O_2$, and $LiMn_2O_4$ nanotubes demonstrated improved electrochemical performance over the particulate forms (Table 1).[29] Polyaniline nanotube arrays (Figure 6c) also showed superior electrochemical properties to the bulk counterpart.[30] Such PANI nanostructures can be applied to Li-polymer thin-film batteries, which are shape-flexible and specifically suitable for powering integrated circuit cards and microelectromechanical systems.

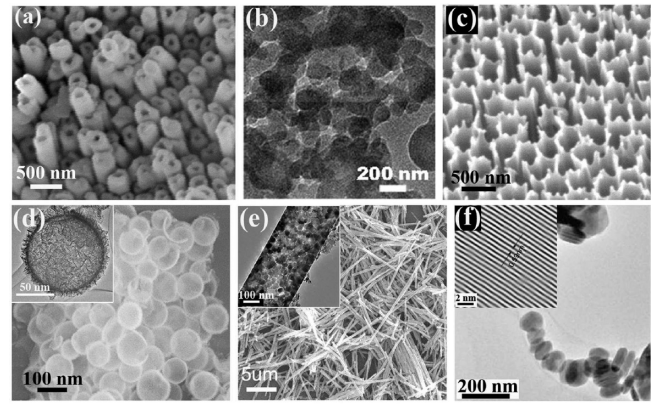

FIGURE 6. SEM and TEM images of nanostructured materials for rechargeable Li ion batteries. Cathode materials: (a) $LiNi_{0.8}Co_{0.2}O_2$ nanotubes, (b) NiP-doped $LiFePO_4$ composite nanoparticles, and (c) poly(aniline) tubular arrays. Anode materials: (d) Si hollow spheres, (e) Co_3O_4 nanotubes, and (f) SnS_2 nanoparticle chains. The insets show magnified images.

TABLE 1. Summary of the Electrode Performance of Typical Nanostructures and Their Particle Counterparts for Rechargeable Li Ion Batteries

	capacity (mA·h/g)			
electrode materials	initial	50th cycle	current density (mA/g)	voltage (V)
$LiNi_{0.8}Co_{0.2}O_2$ nanotube	205	157	10	4.5−3.0
$LiNi_{0.8}Co_{0.2}O_2$ bulk particle	182	143		
$LiFePO_4$ nanoparticle	162	158	50	4.1−2.5
$LiFePO_4$ bulk particle	126	119		
poly(aniline) nanotube	75.7	73.2	20	3.7−2.0
poly(aniline) bulk particle	54	50		
Si porous nanosphere	3052	1095	2000	1.6−0.02
Si bulk particle	1600	52		
Co_3O_4 nanotube	850	530	50	2.80−0.01
Co_3O_4 nanoparticle	635	321		
SnS_2 nanoparticle	1323	390	50	2.75−0.02
SnS_2 bulk particle	979	284		

The potentially cheap and environmentally benign $LiFePO_4$ deserves special attention because it can deliver higher reversible capacity with lower potential (3.4 V vs Li), making it less prone to electrolyte oxidation and safer for use.[31] However, the intrinsic poor conductivity of this material severely limits its practical capacity at high current density. To solve this problem, much effort has been dedicated to reducing the particle size and coating/doping $LiFePO_4$ with a high-conductive component such as carbon layers.[32,33] To take advantage of the nanosize effect, we prepared NiP-doped $LiFePO_4$ composite nanospheres (Figure 6b) through a spraying technique.[34] An approximately 0.9 wt % NiP doping in the nanocomposite increased the conductivity of bulk $LiFePO_4$ by nearly 4 orders of magnitude. Meanwhile, significant improvement of reversible capacity and lithium insertion/extraction kinetics was gained for the doped nanostructures over the undoped microsize particles. Thus, the nanocomposite concept allows simul-

taneously incorporation of short ionic transport distance and enhanced electronic conduction.

Two categories of anode materials have attracted intensive interest as alternative to conventional graphite anode. One is lithium alloy, which has the capability of storing larger quantities of Li than graphite.[35] Typical examples are $Li_{4.4}Si$ (theoretical capacity of 4200 mA·h/g compared with 372 mA·h/g for LiC_6) and $Li_{4.4}Sn$ (993 mA·h/g). The other category is binary metal oxide (e.g., CuO, NiO, Fe_2O_3, and Co_3O_4) based on the so-called conversion reactions: $M_mO_n + 2nLi^+ + 2ne^- \leftrightarrow nLi_2O + mM$, where M represents a 3d transition metal.[36] Unlike theclassic intercalation mechanism, such a transition reaction permits storage of more than two lithium ions per molecule, resulting in significantly higher capacity. Furthermore, this reaction shows satisfactory reversibility, which may be explained by the highly reactive metal nanoparticles embedded in the Li_2O matrix being generated in situ during the initial reduction of metal oxides.

Unfortunately, there are challenges for the above-mentioned two types of high-capacity anode electrodes. For lithium alloys, enormous volume swings could occur during the electrochemical alloy formation. For example, a volume expansion up to 400% was observed during the formation of $Li_{4.4}Si$.[35] Such a huge volume change can cause crack and pulverization of the electrode, leading to rapid capacity deterioration and poor cyclability. Current strategies to overcome this obstacle focus on two aspects: one is reducing the alloy particle size to nanoscale and the other is dispersing Si in a rigid matrix with nanocomposite concept. The major hurdle of the conversion reaction is associated with the large voltage separation between charge and discharge, which results in poor energy efficiency of the electrode. This problem still remains a great challenge facing the widespread practical application of the low-toxicity and cheap metal oxides.

Our attempts to develop high-capacity anode materials focus on Si hollow nanospheres, Fe_2O_3 and Co_3O_4 nanotubes, and SnS_x nanoparticle chains (Figure 6d–f).[37–40] All these peculiar nanostructures exhibit considerable structural flexibility and deliver initial capacities at least two times higher than that of commercially used graphite (Table 1). The initial morphologies of these nanostructures are almost maintained after cycling. In particular, the nest-like Si nanospheres possess unique hollow structures consisting of entwining ultrathin nanowires, which allow fast ionic diffusion and facile strain relaxation and thereby exhibit significantly improved reversible capacity and rate capability compared with their bulk counterparts.

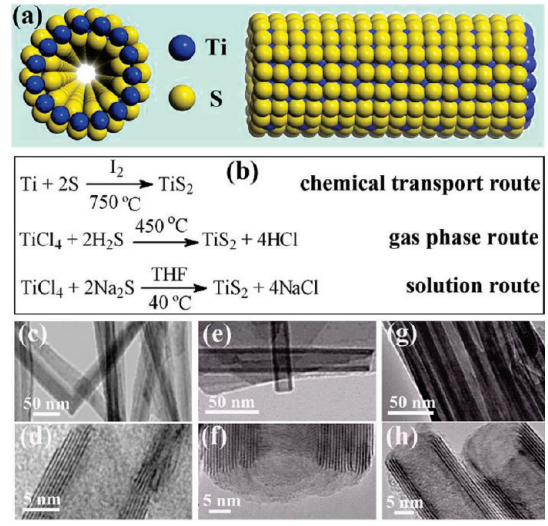

FIGURE 7. (a) Top (left) and side (right) view of TiS_2 tubular structure, (b) synthesis strategy for TiS_2 nanotubes, and TEM images of the nanotubes prepared through (c, d) the chemical transport route, (e, f) the gas phase route, and (g, h) the solution route.

Rechargeable Mg batteries, resembling the Li system in basic operation mechanism, deserve to be mentioned here because they have also received some research interest.[41–43] These batteries typically include components of a Mg metal anode, a Chevrel phase (e.g., $Mg_xMo_6S_8$) cathode, and a Mg organohaloaluminate salt electrolyte in ether solvent.[41] Their advantages arise from the abundance and high energy density of Mg and their impressive cycleability. Some reported results preliminarily showed that nanomaterials were better than the microparticles in facilitating reversible and faster Mg^{2+} intercalation.[42,43] However, their potential application is undermined by the critical usage of complex organic electrolyte and the lack of proper cathode materials with desirable capacity and kinetics.

3.2. TiS_2 and TiO_2 Nanotubes. Inorganic compounds with lamellar structure, such as metal disulfide (MS_2), can adopt nanotubular structures by folding (Figure 7a).[44] Atoms within the S–M–S sheet are bound by strong covalent forces, while individual S–M–S layers are held together by van der Waals interactions. This interlayer gallery offers space and easy access for introduction of foreign ions. The thermodynamic stability and structural flexibility of the nanotubes allow them to undergo repeated diffusion and intercalation of guest items without structure collapse. These features therefore make MS_2 nanotubes useful active materials for storage of lithium and magnesium.[43,45,46]

Special attention is paid to TiS_2 nanotubes because Ti is a lightweight element. High-purity multiwalled TiS_2 nanotubes with uniform open-ended tips can be synthesized through

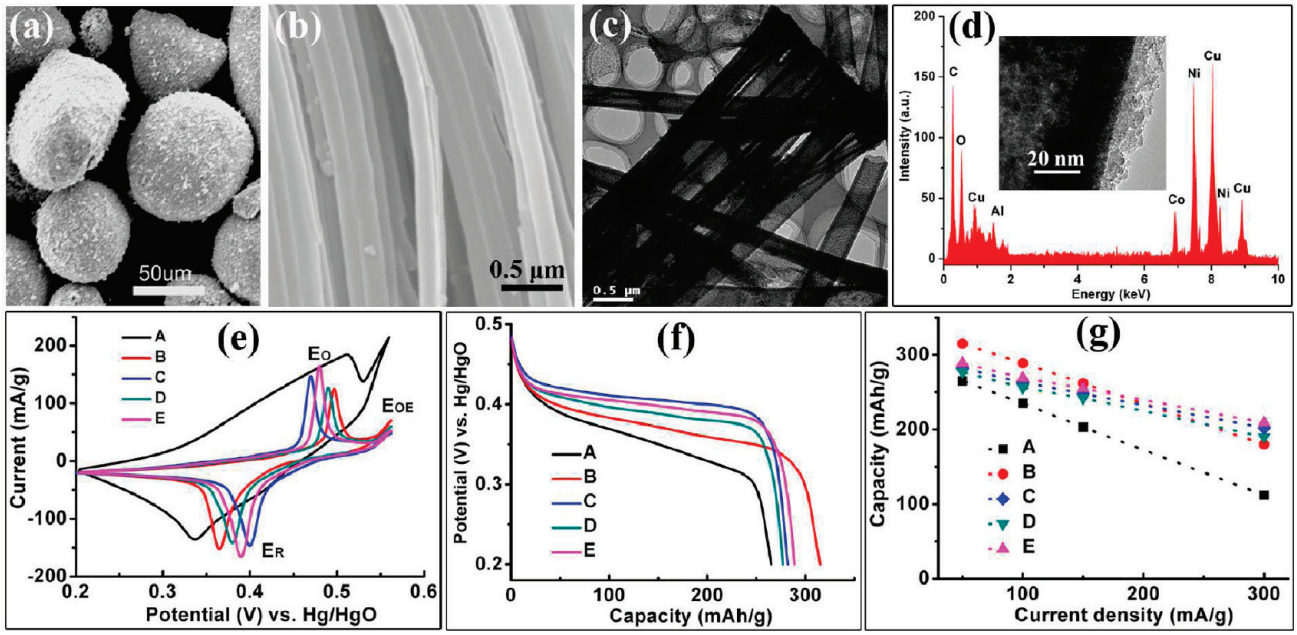

FIGURE 8. $Ni(OH)_2$ for Ni−MH batteries: SEM of $Ni(OH)_2$ (a) bulk particles and (b) nanotubes; (c) TEM and (d) EDX/HRTEM of $Co(OH)_2$-coated $Ni(OH)_2$ tubes; (e) cyclic voltammograms, (f) discharge curve, and (g) high-rate performance of the electrode. A, B, C, D, E correspond to the bulk, pure tubes, and $Y(OH)_3$-coated, $Ca(OH)_2$-coated, and $Co(OH)_2$-coated tubes, respectively.

three strategies (solid, gas, and solution-based routes) using different Ti and S precursors (Figure 7b−h).[46−48] Lithium intercalation into the TiS_2 can be expressed as: $TiS_2 + xLi^+ + xe^- \leftrightarrow Li_xTiS_2$. The essential structure and morphology of TiS_2 nanotubes are maintained after Li intercalation while the lattice parameters of Li_xTiS_2 change slightly with the inserted Li amount x. The possible maximum storage for TiS_2 is up to one lithium atom per molecule. Furthermore, Mg^{2+} can be reversibly intercalated and deintercalated in TiS_2 nanotubes.[46] In a moderate potential range of 2.0−0.5 V, the nanotubes display significantly higher capacity and better rate capability than the polycrystalline powder. Like nanostructured TiS_2, TiO_x nanostructures have also stimulated extensive attention; the synthesis, properties, and applications of nanostructured titanates and TiO_2 can be found in a recent comprehensive review.[49] As illustrative example, TiO_2(B) nanotubes can deliver charge capacity up to 338 mA·h/g (at ~1.5 V vs Li^+/Li) along with excellent rate capability and good cycleability, rendering them as potential anodes for rechargeable Li ion batteries.[50]

3.3. $Ni(OH)_2$-Based Nanotubes for Ni−MH Batteries. Nickel hydroxide is widely used as the cathode material in a series of Ni-based (like Ni−MH, Ni−H, Ni−Cd, Ni−Fe, Ni−Zn) rechargeable batteries. Since the capacities of these batteries are usually cathode-limited, increasing the capacity of the nickel electrode is essential to improve the overall battery performance. The actual electrode reactions participating in the nickel electrode involve structural transition among four types of nickel hydroxides and oxyhydroxides.[2] Because of the Ni^{4+} defects in oxyhydroxides, $Ni(OH)_2$ can yield capacity higher than the theoretical 289 mA·h/g, which is based on one-electron transfer. However, volume expansion/swelling occurs during the phase change, leading to decreased particle contact and increased electrode resistance. This drawback becomes more prominent at high-rate and high-temperature charge/discharge. Traditional approaches to improve the characteristics of nickel electrodes are to introduce additives to spherical powders (Figure 8a). Ionic diffusion and electrolyte contact can occur more easily in hollow tubular structure than in the dense spherical powders.

Generally, the characteristic time (t) for diffusion is determined by $t = L^2/D$, where L is the diffusion length and D the diffusion coefficient.[9] Thus, the tubes with wall thickness of 20−30 nm permit drastically faster transportation of electrons and ions than the bulk particles with diameter of several tens of micrometers. These features endow $Ni(OH)_2$ nanotubes (Figure 8b) with superior electrochemical characteristics compared with the bulk particles.[51] Coating a hydroxide ultrathin layer such as $Ca(OH)_2$, $Co(OH)_2$, or $Y(OH)_3$ on $Ni(OH)_2$ nanotubes (Figure 8c,d) provides further advantages by suppressing the volume change.[52] Cyclic voltammograms (Figure 8e) of the coated electrode display sharp oxidation and reduction peaks, lower current at oxygen-evolution potential (E_{OE}), and decreased separation between oxidation potential (E_O) and

reduction potential (E_R), which indicate improved reaction reversibility. The higher steady voltage plateau in Figure 8f implies enhanced discharge energy efficiency. Furthermore, the composite nanotubes show notable promotion of rate capability (Figure 8g). This example again proves the positive effect of nanostructures on tailoring electrochemical properties of electrode materials.

4. Conclusion and Outlook

The combination of lightweight elements and nanostructured materials has gained not only great academic interest but also high technological value for developing advanced batteries. On one hand, lightweight elements such as hydrogen, lithium, and magnesium are suitable for energy storage and conversion, as they can serve properly either as carriers or as media and can also deliver intrinsic high capacity and energy. On the other hand, shifting from traditional bulk materials to nanostructures provides a new solution to achieve higher capacity and improved rate capability and cyclability. Properties of active materials are found to be size- and shape-dependent. Generally, enhanced electrochemical activity and electrode kinetics arise as particle size decreases. Nanostructures such as nanotubes, nanowires, and porous nanospheres exhibit particular structure flexibility and morphological merits, favoring the electronic and ionic diffusion and transport. Moreover, the selection of active materials has been greatly expanded by using composite nanostructures.

Some intrinsic drawbacks remain to be addressed to fully realize the advantages of nanostructured materials. Up to now, precise control of the size and shape of nanomaterials in mass production is not straightforward. Some elegant top-down and bottom-up strategies have been developed to fabricate novel nanostructures,[53,54] which may shed light on the new synthesis of nanostructured materials for batteries. The low packing density and volumetric energy density is normally considered as another major disadvantage. This hurdle is addressed by developing three dimension (3D) electrodes.[55] Besides, the influence of size effect and surface defects on electrochemical properties needs to be systematically investigated, particularly from the theoretical aspect and the *in situ* analysis. Of course, challenges and opportunities coexist in combining nanostructures and lightweight elements to construct advanced batteries.

We greatly thank our co-workers whose names are listed in the relevant references. We are also grateful to the Projects of National 973 (2005CB623607), NSFC (20873071), and Tianjin Basic Research (08JCZDJC21300).

BIOGRAPHICAL INFORMATION

Jun Chen is a Cheung Kong Professor at Nankai University. He obtained his B.Sc. and M.Sc. degrees from Nankai University in 1989 and 1992, respectively, and his Ph.D. from Wollongong University (Australia) in 1999. He held the NEDO fellowship at National Institute of AIST Kansai Center (Japan) from 1999 to 2002. His research expertise is energy storage & conversion with batteries, fuel cells, and solar cells.

Fangyi Cheng received his B.Sc. and M.Sc. degrees from Nankai University in 2003 and 2006, respectively. He is getting his Ph.D. in 2009 under the supervision of Professor Jun Chen. His research focuses on advanced materials for batteries.

FOOTNOTES

*To whom correspondence should be addressed. Tel/Fax: (+86) 22-23506808. E-mail: chenabc@nankai.edu.cn.

REFERENCES

1 Winter, M.; Brodd, J. B. What are batteries, fuel cells, and supercapacitors? *Chem. Rev.* **2004**, *104*, 4245–4269.
2 Linden, D.; Reddy, T. B. *Handbook of Batteries*, 3rd ed.; McGraw-Hill: New York, 2002.
3 Bard, A. J.; Faulkner, L. R. *Electrochemical Methods: Fundamentals and Applications*; Wiley: New York, 2000.
4 Hu, J.; Odom, T. W.; Lieber, C. M. Chemistry and physics in one dimension: Synthesis and properties of nanowires and nanotubes. *Acc. Chem. Res.* **1999**, *32*, 435–445.
5 Burda, C.; Chen, X.; Narayanan, R.; El-Sayed, M. A. Chemistry and properties of nanocrystals of different shapes. *Chem. Rev.* **2005**, *105*, 1025–1102.
6 Nam, K. T.; Kim, D. W.; Yoo, P. J.; Chiang, C. Y.; Meethong, N.; Hammond, P. T.; Chiang, Y. M.; Belcher, A. M. Virus-enabled synthesis and assembly of nanowires for lithium ion battery electrodes. *Science* **2006**, *312*, 885–888.
7 Aricò, A. S.; Bruce, P.; Scrosati, B.; Tarascon, J. M.; Schalkwijk, W. V. Nanostructured materials for advanced energy conversion and storage devices. *Nat. Mater.* **2005**, *4*, 366–377.
8 Law, M.; Greene, L. E.; Johnson, J. C.; Saykally, R.; Yang, P. D. Nanowire dye-sensitized solar cells. *Nat. Mater.* **2005**, *4*, 455–459.
9 Bruce, P.; Scrosati, B.; Tarascon, J. M. Nanomaterials for rechargeable lithium batteries. *Angew. Chem., Int. Ed.* **2008**, *47*, 2930–2946.
10 Guo, Y.; Hu, J.; Wan, L. Nanostructured materials for electrochemical energy conversion and storage devices. *Adv. Mater.* **2008**, *20*, 2878–2887.
11 Suib, S. L. Porous manganese oxide octahedral molecular sieves and octahedral layered materials. *Acc. Chem. Res.* **2008**, *41*, 479–487.
12 Chabre, Y.; Pannetier, J. Structural and electrochemical properties of the proton/γ-MnO_2 system. *Prog. Solid State Chem.* **1995**, *23*, 1–130.
13 Thackeray, M. M. Manganese oxides for lithium batteries. *Prog. Solid State Chem.* **1997**, *25*, 1–71.
14 Wang, X.; Li, Y. Selected-control hydrothermal synthesis of α- and β-MnO_2 single crystal nanowires. *J. Am. Chem. Soc.* **2002**, *124*, 2880–2881.
15 Cheng, F.; Chen, J.; Gou, X.; Shen, P. High-power alkaline Zn-MnO_2 batteries using γ-MnO_2 nanowires/nanotubes and electrolytic zinc powder. *Adv. Mater.* **2005**, *17*, 2753–2756.
16 Chou, S.; Cheng, F.; Chen, J. Electrodeposition synthesis and electrochemical properties of nanostructured γ-MnO_2 films. *J. Power Sources* **2006**, *162*, 727–734.
17 Cheng, F.; Zhao, J.; Song, W.; Li, C.; Ma, H.; Chen, J.; Shen, P. Facile controlled synthesis of MnO_2 nanostructures of novel shapes and their application in batteries. *Inorg. Chem.* **2006**, *45*, 2038–2044.
18 Jiao, F.; Bruce, P. Mesoporous crystalline β-MnO_2—A reversible positive electrode for rechargeable lithium batteries. *Adv. Mater.* **2007**, *19*, 657–660.
19 Kijima, N.; Yasuda, H.; Sato, T.; Yoshimura, Y. Preparation and characterization of open tunnel oxide α-MnO_2 precipitated by ozone oxidation. *J. Solid State Chem.* **2001**, *159*, 94–102.
20 Sorensen, E. M.; Izumi, H. K.; Vaughey, J. T.; Stern, C. L.; Poeppelmeier, K. R. AgVOF: An electrochemically active and high silver density phase. *J. Am. Chem. Soc.* **2005**, *127*, 6347–6352.

21 Zhang, S.; Li, W.; Li, C.; Chen, J. Synthesis, characterization, and electrochemical properties of $Ag_2V_4O_{11}$ and $AgVO_3$ 1-D nano/microstructures. *J. Phys. Chem. B* **2006**, *110*, 24855–24863.

22 Ma, H.; Zhang, S.; Ji, W.; Tao, Z.; Chen, J. α-CuV_2O_6 nanowires: hydrothermal synthesis and primary lithium battery application. *J. Am. Chem. Soc.* **2008**, *130*, 5361–5367.

23 Balaya, P.; Bhattacharyya, A. J.; Jamnik, J.; Zhukovskii, Y. F.; Kotomin, E. A.; Maier, J. Nano-ionics in the context of lithium batteries. *J. Power Sources* **2006**, *159*, 171–178.

24 Li, W.; Li, C.; Zhou, C.; Ma, H.; Chen, J. Metallic magnesium nano/mesoscale structures: Their shape-controlled preparation and Mg/air battery applications. *Angew. Chem., Int. Ed.* **2006**, *45*, 6009–6012.

25 Ma, H.; Li, C.; Su, Y.; Chen, J. Studies on the vapour-transport synthesis and electrochemical properties of zinc micro-, meso- and nanoscale structures. *J. Mater. Chem.* **2007**, *17*, 684–691.

26 Li, C.; Ji, W.; Chen, J.; Tao, Z. Metallic aluminum nanorods: Synthesis via vapor-deposition and applications in Al/air batteries. *Chem. Mater.* **2007**, *19*, 5812–5814.

27 Whittingham, M. S. Lithium batteries and cathode materials. *Chem. Rev.* **2004**, *104*, 4271–4301.

28 Li, X.; Cheng, F.; Guo, B.; Chen, J. Template-synthesized $LiCoO_2$, $LiMn_2O_4$, and $LiNi_{0.8}Co_{0.2}O_2$ nanotubes as the cathode materials for lithium ion batteries. *J. Phys. Chem. B* **2005**, *109*, 14017–14024.

29 Okubo, M.; Hosono, E.; Kim, J.; Enomoto, M.; Kojima, N.; Kudo, T.; Zhou, H.; Honma, I. Nanosize effect on high-rate Li-ion intercalation in $LiCoO_2$ electrode. *J. Am. Chem. Soc.* **2007**, *129*, 7444–7452.

30 Cheng, F.; Tang, W.; Li, C.; Chen, J.; Liu, H.; Shen, P.; Dou, S. Conducting poly(aniline) nanotubes and nanofibers: Controlled synthesis and application in lithium/poly(aniline) rechargeable batteries. *Chem.—Eur. J.* **2006**, *12*, 3082–3088.

31 Padhi, A. K.; Nanjundaswamy, K. S.; Goodenough, J. B. Phospho-olivines as positive-electrode materials for rechargeable lithium batteries. *J. Electrochem. Soc.* **1997**, *144*, 1188–1194.

32 Huang, H.; Yin, S. C.; Nazar, L. F. Approaching theoretical capacity of $LiFePO_4$ at room temperature and high rates. *Electrochem. Solid-State Lett.* **2001**, *4*, A170—A172.

33 Chuang, S. Y.; Bloking, J. T.; Chiang, Y. M. Electronically conductive phospho-olivines as lithium storage electrodes. *Nat. Mater.* **2002**, *1*, 123–128.

34 Li, C.; Zhang, S.; Cheng, F.; Ji, W.; Chen, J. Porous $LiFePO_4$/NiP composite nanospheres as the cathode materials in rechargeable lithium-ion batteries. *Nano Res.* **2008**, *1*, 242–248.

35 Kasavajjula, U.; Wang, C.; Appleby, A. J. Nano- and bulk-silicon-based insertion anodes for lithium-ion secondary cells. *J. Power Sources* **2007**, *163*, 1003–1039.

36 Poizot, P.; Laruelle, S.; Grugeon, S.; Dupont, L.; Tarascon, J. M. Nano-sized transition-metal oxides as negative-electrode materials for lithium-ion batteries. *Nature* **2000**, *407*, 496–499.

37 Ma, H.; Cheng, F.; Chen, J.; Zhao, J.; Li, C.; Tao, Z.; Liang, J. Nest-like silicon nanospheres for high-capacity lithium storage. *Adv. Mater.* **2007**, *19*, 4067–4070.

38 Chen, J.; Xu, L.; Li, W.; Gou, X. α-Fe_2O_3 nanotubes in gas sensor and lithium-ion battery applications. *Adv. Mater.* **2005**, *17*, 582–586.

39 Li, W.; Xu, L.; Chen, J. Co_3O_4 nanomaterials in lithium-ion batteries and gas sensors. *Adv. Funct. Mater.* **2005**, *15*, 851–857.

40 Gou, X.; Chen, J.; Shen, P. Synthesis, characterization and application of SnS_x ($x = 1,2$) nanoparticles. *Mater. Chem. Phys.* **2005**, *93*, 557–566.

41 Aurbach, D.; Lu, Z.; Schechter, A.; Gofer, Y.; Gizbar, H.; Turgeman, R.; Cohen, Y.; Moshkovich, M.; Levi, E. Prototype systems for rechargeable magnesium batteries. *Nature* **2000**, *407*, 724–727.

42 Aurbach, D.; Suresh, G. S.; Levi, E.; Mitelman, A.; Mizrahi, O.; Chusid, O.; Brunelli, M. Progress in rechargeable magnesium battery technology. *Adv. Mater.* **2007**, *19*, 4260–4267.

43 Tao, Z.; Xu, L.; Gou, X.; Chen, J.; Yuan, H. TiS_2 nanotubes as the cathode materials of Mg-ion batteries. *Chem. Commun.* **2004**, 2080–2081.

44 Tenne, R. Inorganic nanotubes and fullerene-like nanoparticles. *Nat. Nanotechnol.* **2006**, *1*, 103–111.

45 Zak, A.; Feldman, Y.; Lyakhovitskaya, V.; Leitus, G.; Popovitz-Biro, R.; Wachtel, E.; Cohen, H.; Reich, S.; Tenne, R. Alkali metal intercalated fullerene-like MS_2 (M = W, Mo) nanoparticles and their properties. *J. Am. Chem. Soc.* **2002**, *124*, 4747–4758.

46 Chen, J.; Tao, Z.; Li, S. Lithium intercalation in open-ended TiS_2 nanotubes. *Angew. Chem., Int. Ed.* **2003**, *42*, 2147–2151.

47 Chen, J.; Li, S.; Tao, Z.; Gao, F. Low-temperature synthesis of titanium disulfide nanotubes. *Chem. Commun.* **2003**, 980–981.

48 Chen, J.; Li, S.; Tao, Z.; Shen, Y.; Cui, C. Titanium disulfide nanotubes as hydrogen-storage materials. *J. Am. Chem. Soc.* **2003**, *125*, 5284–5285.

49 Bavykin, D. V.; Friedrich, J. M.; Walsh, F. C. Protonated titanates and TiO_2 nanostructured materials: Synthesis, properties, and applications. *Adv. Mater.* **2006**, *18*, 2807–2824.

50 Armstrong, G.; Armstrong, A. R.; Canales, J.; Bruce, P. G. TiO_2(B) nanotubes as negative electrodes for rechargeable lithium batteries. *Electrochem. Solid-State Lett.* **2006**, *9*, A139—A143.

51 Cai, F.; Zhang, G.; Chen, J.; Gou, X.; Liu, H.; Dou, S. $Ni(OH)_2$ tubes with mesoscale dimensions as positive-electrode materials for alkaline rechargeable batteries. *Angew. Chem., Int. Ed.* **2004**, *43*, 4212–4216.

52 Li, W.; Zhang, S.; Chen, J. Synthesis, characterization, and electrochemical application of $Ca(OH)_2$-, $Co(OH)_2$-, and $Y(OH)_3$-coated $Ni(OH)_2$ tubes. *J. Phys. Chem. B* **2005**, *109*, 14025–14032.

53 Tao, A. R.; Huang, J.; Yang, P. Langmuir—Blodgettry of nanocrystals and nanowires. *Acc. Chem. Res.* **2008**, *41*, 1662–1673.

54 Xu, Q.; Rioux, R. M.; Dickey, M. D.; Whitesides, G. M. Nanoskiving: A new method to produce arrays of nanostructures. *Acc. Chem. Res.* **2008**, *41*, 1566–1577.

55 Long, J. W.; Dunn, B.; Rolison, D. R.; White, H. S. Three-dimensional battery architectures. *Chem. Rev.* **2004**, *104*, 4463–4492.